

# IR-Spectroscopic Characterization of Acetophenone Complexes with Fe<sup>+</sup>, Co<sup>+</sup>, and Ni<sup>+</sup> Using Free-Electron-Laser IRMPD<sup>†</sup>

Robert C. Dunbar,<sup>\*,‡</sup> David T. Moore,<sup>§</sup> and Jos Oomens<sup>§</sup>

Department of Chemistry, Case Western Reserve University, Cleveland, Ohio 44106, and FOM Institute for Plasma Physics “Rijnhuizen”, Edisonbaan 14, 3439MN Nieuwegein, The Netherlands

Received: November 18, 2005; In Final Form: January 25, 2006

The gas-phase complexes M<sup>+</sup>(acet)<sub>2</sub>, where M is Fe, Co, or Ni and acet is acetophenone, were studied spectroscopically by infrared multiple-photon dissociation (IRMPD) supported by density functional (DFT) computations. The FELIX free electron laser was used to give tunable radiation from ~500 to 2200 cm<sup>-1</sup>. The spectra were interpreted to determine the metal-ion binding sites on the ligands (oxygen (O) or ring (R)) and to see if rearrangement of the ligand(s) to toluene plus CO occurred. For Ni<sup>+</sup>, O binding was found to predominate (similar to the previously studied Cr<sup>+</sup> case), with less than ~10% of R-bound ligands in the population. For Co<sup>+</sup>, a roughly equal mixture of R-bound and O-bound ligands was present; based on the computed thermochemistry, the OR complex was considered likely to predominate. Fe<sup>+</sup> complexes appeared largely O-bound, but with clear evidence for some R-binding. The exceptionally large extent of R binding for Co<sup>+</sup> highlights the special affinity of this metal ion for aromatic ring ligands. In contrast, the predominant O binding for Ni<sup>+</sup> emphasizes the especially high metal-ion affinity of the O site of acetophenone compared with other ligands such as anisole where R binding of Ni<sup>+</sup> predominates. The spectra did not indicate significant intracomplex rearrangement of ligands to toluene plus CO, and in particular for the Co<sup>+</sup> case the absence of a metal-bound C≡O stretching peak near 2100 cm<sup>-1</sup> strongly ruled out such a rearrangement.

## Introduction

The late first-row transition metal ions complex strongly with aromatic ligands, with benzene receiving the most attention as the prototypical case.<sup>1–5</sup> For other aromatic ligands offering multiple binding functionality, such as an n-donor moiety like an amino or keto-group, these alternative binding sites can compete with the aromatic site for metal ions.<sup>6,7</sup> Understanding the binding of transition metal ions to these different moieties is of interest for elucidating fundamental phenomena like metal–ligand interactions and metal-ion solvation.<sup>8–11</sup> Competition between aromatic  $\pi$  binding sites and electronegative-atom n-donor sites for metal ion binding has broader interest in view of the widespread occurrence of both of these types of binding sites in common biomolecules such as polypeptides and proteins.<sup>12–16</sup> For example, it is known that the presence of metal ions can drastically affect the folding of proteins, changing both secondary and tertiary structures. Common examples of this are iron in hemoglobin and also zinc finger proteins. In many other important cases, such as photosynthesis and electron transport,<sup>17,18</sup> DNA binding,<sup>19</sup> and the activities of some therapeutic agents,<sup>20,21</sup> transition metals bound in coordination complexes with aromatic or n-donor ligands play an important role in determining both structure and function of the biological systems.

In previous work, we have considered the ability of alkoxy, amino, and carbonyl side chains to compete with aromatic sites for the Cr<sup>+</sup> ion.<sup>7</sup> Only the carbonyl oxygen of acetophenone was found to provide a more attractive binding site than the

benzene ring for this metal ion. Based on binding energy measurements from threshold collision induced dissociation (TCID) studies,<sup>3,22</sup> the late transition metal ions Fe<sup>+</sup>, Co<sup>+</sup>, and Ni<sup>+</sup> have stronger affinities for the aromatic ring than Cr<sup>+</sup>. Thus, it is a real possibility that aromatic sites would be preferred binding sites for these ions on acetophenone, even in competition with the carbonyl oxygen. The present work explores these possibilities for the bis complexes of acetophenone with these three metal ions. The Co<sup>+</sup> system has particular interest, because this metal ion has exceptional affinity for  $\pi$  binding to aromatic rings,<sup>1,3,4,6</sup> whereas acetophenone is exceptional among bifunctional  $\pi/n$  ligands in offering particularly high metal ion affinity at the n (oxygen) site.<sup>7</sup> Balancing these factors, it is hard to predict the favored geometry of the Co<sup>+</sup>/acetophenone complexes, so that these systems offer an attractive opportunity for experimental differentiation using new spectroscopic approaches.

Newly emerging techniques of gas-phase ion spectroscopy exploiting intense tunable infrared (IR) light sources make possible the in situ characterization of ionic complexes in the gas phase.<sup>2,7,23–35</sup> The direct structural information coming from this IR spectroscopy, when compared against computationally predicted spectra, can allow one to distinguish the preferred sites of complexation,<sup>7,34</sup> to gain insights into the rearrangement chemistry that may accompany metal ion complexation,<sup>30,32,33,36</sup> and even to distinguish spin states of the complexed metal ion.<sup>7,30</sup> Since it is not generally possible to measure the IR direct absorption spectra of trapped gas-phase ions, the process of infrared multiple-photon dissociation (IRMPD) is used in this work as an indirect “action spectroscopy” approach for obtaining spectra which have been shown to be good surrogates for the linear absorption spectra.<sup>37</sup> This method employs an intense infrared laser to resonantly pump vibrational energy into the

<sup>†</sup> Part of the “Chava Lifshitz Memorial Issue”.

<sup>\*</sup> To whom correspondence should be addressed.

<sup>‡</sup> Case Western Reserve University.

<sup>§</sup> FOM.

**TABLE 1: Energies of Bis Complexes Relative to  $M^+$  + Separate Ligands ( $\text{kJ mol}^{-1}$ )**

	$\text{Cr}^b$	Fe	Co	Ni
(benzene) <sub>2</sub> <sup>a</sup>	402	395	423	390
RR	295 (D)	373 ( $D = 369$ ) <sup>c</sup>	426	387
OO	421	447	448	472
OR	323	414 ( $D=332$ ) <sup>c</sup>	447	438
AcetTolCO (O)	332	461	474	476
AcetTolCO (R)		442	426	422

<sup>a</sup> Sum of experimental binding energies for two benzene ligands from ref 3. <sup>b</sup> Acetophenone values for  $\text{Cr}^+$  from calculations reported in ref 7. <sup>c</sup> Entries labeled D are doublet states, while the other  $\text{Fe}^+$  values are quartet states.

molecule in a noncoherent fashion, until it has sufficient energy to dissociate.<sup>37,38</sup>

The thermochemistry of binding of first-row transition metals to benzene is well established,<sup>3</sup> providing a model for the binding of metal ions to the ring of acetophenone (Table 1). The later transition metal ions all favor a high-spin  $3d^{n-1}4s^1$  configuration in the absence of ligands, but the presence of a ligand field usually promotes the ion into a  $3d^n$  configuration, so that the configurations of interest here are  $\text{Fe}^+$  ( $3d^7$ ),  $\text{Co}^+$  ( $3d^8$ ), and  $\text{Ni}^+$  ( $3d^9$ ). As is well understood,<sup>1</sup>  $\text{Co}^+$  gives the strongest ring  $\pi$  bonding among the late transition metals, because its  $d^8$  configuration allows double occupation of the  $d \rightarrow \pi^*$  metal-to-ligand donor orbitals ( $d_{xy}$  and  $d_{x^2-y^2}$ ) as well as the weakly interacting  $d_z^2$  orbital, while at the same time allowing single occupation of the two metal orbitals ( $d_{xz}$  and  $d_{yz}$ ) that are subject to repulsive interaction with the filled ligand  $\pi$  orbitals. Both  $\text{Fe}^+$  and  $\text{Ni}^+$  have weaker (though still strong)  $\pi$  binding ability. In the case of  $\text{Ni}^+$ , the weaker binding is a consequence of the addition of one  $d-\pi$  repulsive electron in the  $d$  shell.<sup>1</sup> The stronger binding in the  $\text{Co}^+$  complex relative to the  $\text{Fe}^+$  complex is attributed, by Bauschlicher et al.,<sup>1</sup> to a greater extent of  $d-\pi^*$  back-donation in the  $\text{Co}^+$  system. On the basis of these qualitative considerations, we may anticipate that among late transition metal ions  $\text{Co}^+$  will compete most favorably for the  $\pi$  site compared with the O site of acetophenone.

Much less information is available on the binding of carbonyl moieties to transition metal ions. The only value found in the literature is an estimate of 209 kJ/mol for the acetone- $\text{Co}^+$  complex, which was estimated on the basis of available thermochemical values for similar systems.<sup>39</sup> On the other hand, the reactions of ketones and aldehydes with late transition metal ions have been studied rather extensively.<sup>39-44</sup> For smaller systems such as acetone, the primary mode of reaction is decarbonylation, producing a CO molecule and the corresponding alkane,<sup>39,40</sup> although a richer chemistry is observed for the larger ketones and aldehydes.<sup>41,43</sup> Unfortunately, acetophenone was not included in any of these earlier studies, although one might reasonably expect it to behave similarly to the smaller ketones and undergo decarbonylation to produce metal-ion bound toluene.

The extent of the catalytic activity of later transition metal ions for the decarbonylation of small ketones is illustrated by the kinetic energy release distribution (KERD) measurements from the Bowers group, which were consistent with the rate-determining transition states for decarbonylation lying below the asymptotic reactant energy.<sup>40</sup> This raises the interesting possibility that the  $M^+$ /acetophenone bis complexes studied here may have available an intracomplex rearrangement reaction, making accessible both the expected "reactant-side" bis-acetophenone complex structures, and also the "product-side"

ternary complex structures with acetophenone, toluene, and CO as ligands on the metal ion. It is expected that this would show up in the spectroscopy of these systems, and this question is addressed below.

## Experimental Section

The experimental apparatus, based on the coupling of a 4.7 T Fourier transform ion cyclotron resonance (FT-ICR) mass spectrometer with the beam line of the FELIX free electron laser, has been discussed in detail elsewhere.<sup>27,45</sup> Briefly, metal ions are generated via laser ablation from sputtering targets (Goodfellow, 99.98% purity) using single pulses ( $\sim 20$  mJ) from an Nd:YAG laser (EKSPLA). The ions then drift into the ICR cell, where they are trapped and exposed to a pulse of acetophenone vapor ( $5-10 \times 10^{-7}$  Torr peak pressure) in order to form the complexes. A second pulse of He gas ( $\sim 5 \times 10^{-6}$  Torr peak pressure) is also used to help stabilize the complexes. The acetophenone (Aldrich, 99%) was used as received from the supplier, except for a freeze-pump-thaw cycle to remove dissolved gases. A reaction delay of 3-5 s was used to allow the complexes of interest to form and cool via collisions (in the presence of the decaying pulses of He and of acetophenone) and via spontaneous emission<sup>46</sup> toward the ambient temperature in the ICR trap, namely 300 K. Since laser ablation is known to produce significant abundances of metal atoms and ions in excited electronic states,<sup>47</sup> such a delay was considered necessary to ensure that the complexes were in the ground electronic state when the spectra were taken. Under these conditions, only bis-acetophenone complexes (along with substantial amounts of mono-decarbonylated bis complexes) were observed in abundance, although small amounts of mono and tris complexes were also seen in the final ion populations. The reaction sequences leading to the bis complexes were not explicitly elucidated in these experiments. Sequential reactions leading to  $\text{ML}_2^+$  are normal for transition-metal ions reacting with carbonyl compounds in the FT-ICR cell.<sup>42</sup>

After the ion-molecule reactions, the complexes of interest were isolated and irradiated with several (typically 10) pulses from FELIX. Each FELIX pulse ( $\sim 7 \mu\text{s}$ ) consists of a 1 GHz train of micropulses ( $\sim 10 \mu\text{J}$  energy), and the duration of these micropulses ( $\sim 1$  ps) determines the bandwidth of the radiation, which is typically 0.2-0.5% of the central wavelength. The wavelength is continuously tunable between 3 and 250  $\mu\text{m}$ ; in this work, we investigated the range between 500 and 2200  $\text{cm}^{-1}$  (20-4.5  $\mu\text{m}$ ). Upon resonant absorption of multiple photons, the complex can reach internal energies beyond the dissociation threshold and hence undergo fragmentation. After irradiation with FELIX, a standard FT-ICR excite/detect event<sup>48</sup> was applied to determine the extent of photodissociation. Several photofragment channels were observed for each complex, including loss of intact ligands and decarbonylation. Some significant differences between the spectra in the different channels were observed (see below); however, it is generally most appropriate to use the sum of all fragment channels to represent the absorption of the parent complex under study. Therefore, unless otherwise noted, the infrared (IRMPD) spectra presented herein represent the total fragmentation of the parent complexes, plotted as a function of the wavelength of FELIX. The extent of fragmentation was typically  $\sim 20\%$  for the most intense peaks.

**Comparison with Calculations.** The thermochemistry and harmonic vibrational modes of the complexes were calculated by DFT/MPW1PW91 using Gaussian 03.<sup>49</sup> Computational protocols were similar to those described previously.<sup>7</sup> The

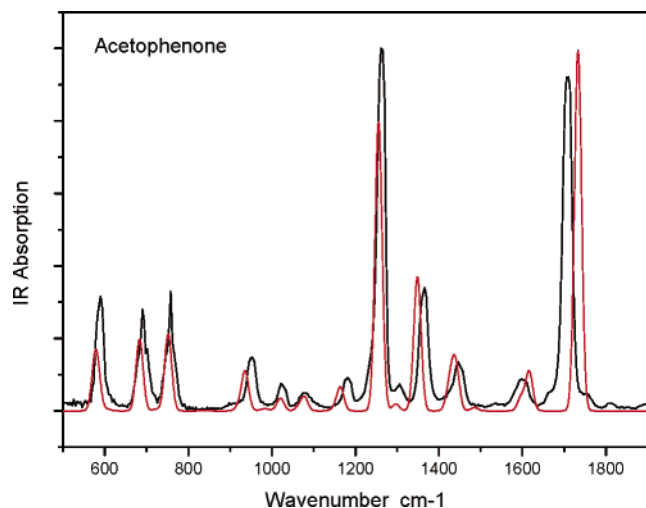


**Figure 1.** IR absorption spectrum of acetophenone neutral<sup>50</sup> compared with DFT calculation using the present protocol.

calculated harmonic normal-mode frequencies were scaled by 0.965. This scaling factor gives a very good fit to the major peaks in the IR spectrum of neutral acetophenone (Figure 1) and is similar to the scaling factors that have been adopted in other DFT fits of IRMPD spectra of first-row transition metal complexes.<sup>7,29</sup> The figure typifies the generally excellent agreement of computations at this level with IR absorption spectra. In the figures, the calculated vibrational stick spectra were convoluted with a Gaussian line shape function with a full width at half-maximum of 20 cm<sup>-1</sup> for Figure 1 and 30 cm<sup>-1</sup> for the other figures.

The C=O stretching mode near 1750 cm<sup>-1</sup>, which is important as a highly diagnostic feature for ring-bound metal ions, shows slightly unsatisfactory behavior in our studies of acetophenone complex spectra, in that this peak appears lower than predicted by amounts ranging from 20 to 53 cm<sup>-1</sup>. Neither using larger basis sets nor using the alternative B3LYP functional gives any apparent improvement. This disagreement of calculation and observation is larger than has been found typical for the frequency correlations of theory and experiment both in the other peaks of the present spectra and in other IRMPD studies of gas-phase ions. This could raise concern about whether the structure assignments of ring-bound acetophenone ligands in the present study are correct. However, it appears that this vibration is not well treated by the present DFT protocol, since the predicted value for this mode is also considerably too low (by 25 cm<sup>-1</sup>) for neutral acetophenone (Figure 1), where there is no possibility of a wrong structural assignment. We place confidence in the use of this peak as a diagnostic feature of ring-bound acetophenone complexes, particularly because of its relatively isolated location in the spectra, and we attribute the consistent under-prediction of this frequency to problems with the DFT treatment.

Judging (very approximately) from peaks in the spectra that appear to be isolated single transitions, we estimate the line widths as typically 30 cm<sup>-1</sup>, which is similar to what was reported as typical for IRMPD spectra of some medium-sized PAH ions.<sup>37</sup> The spectra of the complexes also show evidence of varying amounts of congestion, particularly in the 1100–1500 cm<sup>-1</sup> region (minimal for Cr, increasingly substantial for Ni and Co, and most severe for Fe). Lending support to this suggestion are recently described results on an analogous system:<sup>29</sup> a spectrum of the K<sup>+</sup>(phenylalanine) complex showed similar heavy congestion in this region, which was greatly reduced in a later spectrum of Ag<sup>+</sup>(phenylalanine) employing

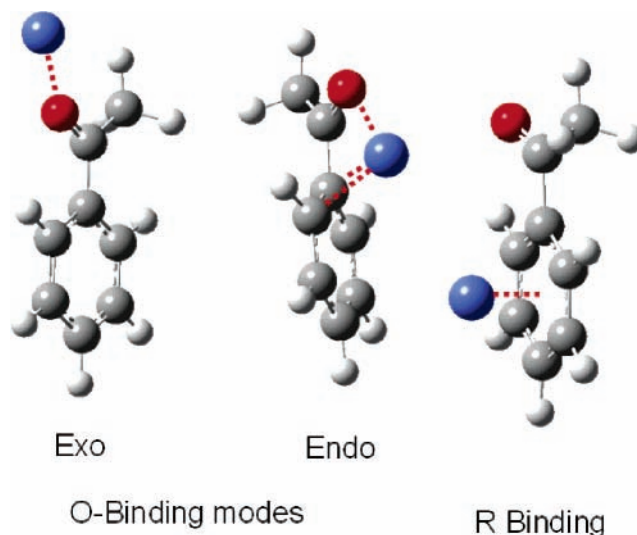


**Figure 2.** Metal ion binding motifs for acetophenone.

a more effective ion thermalization technique. We may note that the same experimental parameters (timings, FEL power, number of FEL shots) were used for all of the metals, and all of the new spectra (Fe<sup>+</sup>, Co<sup>+</sup> and Ni<sup>+</sup> complexes) were recorded on the same day. However, it is worth noting that for the Fe<sup>+</sup> complexes it was more difficult to maintain a stable ion signal, and this contributed to the somewhat decreased signal-to-noise ratio in that spectrum.

## Results and Discussion

**Binding Modes.** Four low-energy binding motifs were identified as available to each of the two acetophenone ligands. Two of these, designated R and O<sub>exo</sub> in Figure 2, are expected modes of attachment to the basically undistorted ligand. A third binding geometry, not pictured, is the in-plane O-binding site (“planar endo”) on the endo side of the oxygen, which was consistently found as a local potential energy minimum. This latter binding geometry in both mono- and bis-complexes was generally calculated as less stable by amounts ranging from 10 to 25 kJ/mol than the corresponding O<sub>exo</sub> geometry and also (with one or two possible exceptions) less stable than the O<sub>endo</sub> geometry. Since it is less stable than O<sub>exo</sub> and O<sub>endo</sub>, offers no apparent steric or other advantages in forming the bis-complexes, and probably rearranges with small barrier to O<sub>endo</sub>, it was not taken into consideration in cataloging the likely geometries of the bis complexes.

The fourth binding motif, the chelated form O<sub>endo</sub> (Figure 2), is interesting in that it moves the acetyl group out of planarity with the benzene ring, thereby sacrificing some resonance stabilization of the ligand moiety in exchange for the advantage of chelating the metal ion between the oxygen and an η<sup>2</sup> interaction with the ring. This O<sub>endo</sub> geometry is shown in Figure 2. Interestingly, O<sub>endo</sub> is calculated to be the most stable geometry for all three of the mono complexes of the present late transition metal ions (but not for the Cr<sup>+</sup> complex, which spontaneously rearranges to the planar-endo complex). However, the chelated O<sub>endo</sub> binding motif is less favorable when two ligands share the metal coordination shell, and the bis-complexes with two O<sub>exo</sub> ligands are consistently predicted to be more stable by amounts of the order of 10–20 kJ mol<sup>-1</sup> than those containing one or two O<sub>endo</sub> ligands. Moreover, the vibrational calculations consistently predicted spectra for the O<sub>exo</sub> and O<sub>endo</sub> isomers that were too similar for the isomers to be distinguished on the basis of the present spectroscopy. Accordingly, we will

base the following discussion on the assumption that the O-bound complexes have the  $O_{\text{exo}}$  geometry but bearing in mind that the present spectroscopic results do not actually distinguish this from the  $O_{\text{endo}}$  alternative.

**Calculated Thermochemistry.** Table 1 summarizes relevant aspects of the thermochemistry of these systems. A useful reference point for considering ring-bound complexes is the experimental threshold collision induced dissociation (TCID) values for benzene.<sup>3</sup> To facilitate comparison of the present results with that study, the summed first and second ligand binding energies are included in the first row of Table 1. With the exception of  $\text{Cr}^+$  (see below), the calculated total binding energies for the acetophenone complexes with exclusively  $\pi$ -bound ligands are nicely parallel to the experimental values for the benzene complexes. In particular, the  $\text{Co}^+$  complex shows significantly higher affinity for ring-binding than either  $\text{Fe}^+$  or  $\text{Ni}^+$ , as expected from the qualitative orbital interaction arguments noted in the Introduction. Note that the  $\text{Fe}^+$  RR bis complex could have either a doublet or quartet ground state; the calculated stabilities of these are the same within the expected uncertainty of the calculations.

The OO complexes of the three late transition metals are not very different from each other in stability. The combination of this with the RR trends leads to the predictions that OO binding should be strongly favored for  $\text{Fe}^+$  and  $\text{Ni}^+$ , but the ring and oxygen sites should be more competitive with each other for  $\text{Co}^+$ . For this latter metal ion, the OR complex is calculated to be essentially equal to the OO complex, indicating equality within the computational uncertainty of the ring and O sites. The RR complex might be expected to be similar but is actually calculated to have somewhat lower stability, perhaps because of some steric repulsion of the two ring-bound ligands. For  $\text{Ni}^+$  and  $\text{Fe}^+$ , it is clear that ring binding is much less favorable than O binding. In general, the table suggests that each switch of a ligand from R binding to O binding gains  $\sim 40 \text{ kJ mol}^{-1}$  in stability for these two ions.

Finally, the rearrangement to the intracomplex decarbonylation structure  $\text{M}^+(\text{acet})(\text{toluene})(\text{CO})$  was found to give the most globally stable structure for all three late transition metal ions, but for  $\text{Fe}^+$  and  $\text{Ni}^+$ , the energy gains from the decarbonylation rearrangement are not as strong as for  $\text{Co}^+$ . The intracomplex decarbonylation reaction for  $\text{Co}^+(\text{acet})_2$  is thermochemically quite favorable.

There is an unresolved uncertainty in the binding thermochemistry of the benzene bis complex with  $\text{Cr}^+$ . To the extent that this may reflect an uncertainty in the DFT-calculated thermochemistry, it could have bearing on the present thermochemical predictions. The problem is that DFT calculations for  $\text{Cr}(\text{Bz})_2^{+2}$  are lower by a large amount ( $\sim 1 \text{ eV}$ ) than the barrier to second-ligand removal obtained by credible kinetic modeling of experimental results from two different techniques.<sup>3,51</sup> It has been speculated that this discrepancy is connected with the change in spin between the doublet bis-complex and the sextet mono-complex, but it remains unclear whether the problem lies with the experiments, the kinetic modeling, the DFT calculations, or some combination of these.<sup>3,7,51</sup> Fortunately, benzene bis complexes of other transition metal ions do not seem to share this problem, since the DFT calculations of both the first and second ligand binding energies of benzene to  $\text{Fe}^+$ ,  $\text{Co}^+$ , and  $\text{Ni}^+$  are within 3 kcal/mol of the experimental values.<sup>2</sup> Furthermore, our previous study of aniline and anisole with  $\text{Cr}^+$  showed that, irrespective of any possible problems in calculation of the thermochemistry, DFT vibrational calculations of the

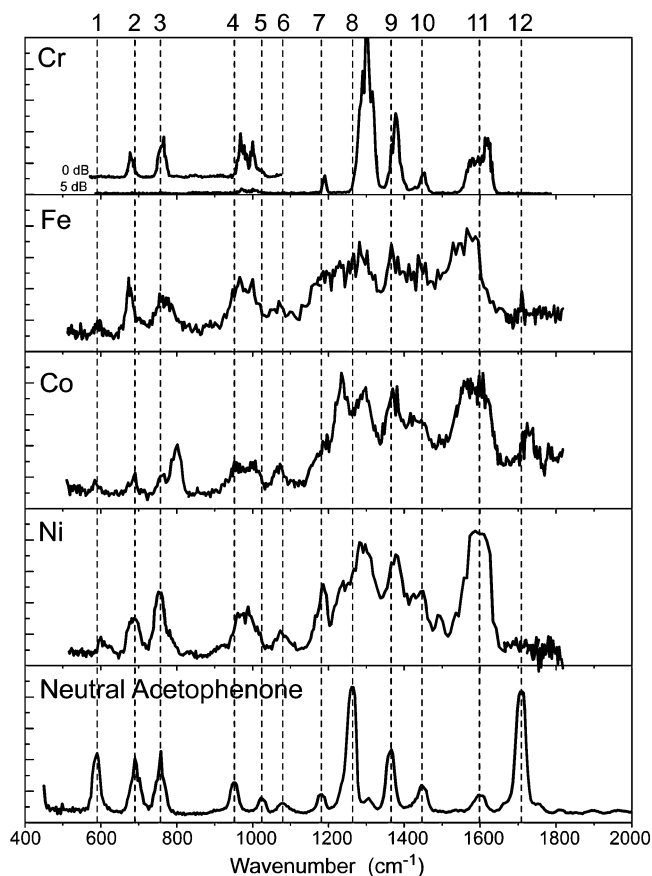


**Figure 3.** Felix IRMPD spectra of the four measured  $\text{M}^+(\text{acet})_2$  complexes (present results and ref 7 along with the IR absorption spectrum of the neutral ligand<sup>50</sup>). Blue lines and corresponding labels at the top provide indexing for 12 of the prominent peaks in the neutral acetophenone spectrum.

doublet states of the RR bis-complexes produced predicted spectra that agreed well with the IRMPD results.<sup>7</sup>

**Spectroscopic Results.** The spectra and their interpretations are not straightforward, and it is instructive to start the analysis with a comprehensive comparison of all of the measured  $\text{M}^+(\text{acet})_2$  spectra, along with the IR absorption spectrum of the neutral ligand.<sup>50</sup> These are shown in Figure 3. It is immediately clear that the ion spectra are similar in many of their features but that there are also significant differences among them and also between them and the neutral ligand. Inspection of the similarities and differences leads to a convincing assignment of the conformations and spectra of the ions.

The correlation and interpretation of these spectra are described using (dashed) index lines added on Figure 3, along with the numbers labeling 12 clear features of the neutral-ligand spectrum. The normal mode character of each of these 12 features, as indicated from the calculations, is described in Table 2. The most intense modes in the neutral spectrum are peaks 8 (ring to side chain C–C stretch) and 12 (CO stretch), which is fortunate, since they correspond to modes that are quite sensitive to the particular site of metal ion binding and hence are the most useful diagnostic features. Peak 3 (out-of-plane ring CH bend) is also a possibly useful diagnostic peak, since it is fairly well isolated in the spectrum and corresponds to a mode that has been shown for other aromatic ligands to blueshift in the presence of ring-bound transition metal ions.<sup>2,7</sup> Peak 9 (methyl umbrella and C–C stretch) is a fairly intense mode that is perturbed by side chain binding. Peak 11 corresponds to the IR-active C–C stretching deformation modes of the aromatic

**TABLE 2: Principal IR Absorption Peaks of the Neutral Ligand Visible in Figure 1, Along with the Normal Mode Characteristics Indicated by the DFT Calculations**

peak #	neutral ligand frequency (cm <sup>-1</sup> )	mode character <sup>a</sup>
1	590	ip C=O bend
2	691	ring oop CH bend
3	757	ring oop CH bend
4	952	CH <sub>3</sub> rock
5	1024	ip ring deformation
6	1080	ip ring H bend
7	1182	ip ring H bend
8	1263	ring-side-chain C–C stretch
9	1366	OC–CH <sub>3</sub> C–C stretch and CH <sub>3</sub> umbrella
10	1446	CH <sub>3</sub> scissors and ip ring H bend
11	1598	ip ring deformation
12	1708	C=O stretch

<sup>a</sup> ip = in-plane; oop = out-of-plane.

ring, which were useful diagnostic modes for complexes of aniline and anisole in our earlier study.<sup>7</sup> This is a less useful feature for acetophenone however, since it is weaker in general and is also overlapped by (redshifted) peak 12 in some cases (see below). The rest of the spectrum seems to consist of “spectator” modes which are similar in position and intensity in all spectra, regardless of metal ion binding site.

The spectrum of the Cr<sup>+</sup> complex was interpreted in our earlier work<sup>7</sup> as reflecting pure OO binding, and this interpretation still seems valid. The CO stretching mode (peak 12) is strongly redshifted to ~1600 cm<sup>-1</sup>, as expected when the metal ion binds to the carbonyl group, and there is no sign of any “free” carbonyl stretch near 1700 cm<sup>-1</sup>, which would be expected for ring bound ligands. Furthermore, the overall fit of the experimental spectrum of the Cr<sup>+</sup> complex to the calculated spectrum of the OO bound bis complex was shown to be quite good.<sup>7</sup> The IRMPD spectrum of the Ni<sup>+</sup> complex is qualitatively quite similar to that of Cr<sup>+</sup>, although it appears somewhat broadened and more congested. We take this as a strong indication that the acetophenone ligands in the Ni<sup>+</sup> complexes are predominantly O-bound as well, although there is some evidence for a small population of R-bound ligands, as discussed below.

The Co<sup>+</sup> spectrum has peaks that correspond nicely to the major features of the Cr<sup>+</sup> and Ni<sup>+</sup> spectra, but it also shows three additional peaks at 1720, 1230, and 800 cm<sup>-1</sup>. The first of these corresponds to an unperturbed carbonyl stretch (peak 12) and thus is strongly indicative of ring binding, as discussed above. Similarly, the peak at 800 cm<sup>-1</sup> is consistent with a blue-shifted out-of-plane (oop) C–H bending mode of the aromatic ring (peak 3), another indicator of ring binding. The assignment of the peak at 1230 cm<sup>-1</sup> is not as readily apparent, but the computational data (see below) indicate that it corresponds to red-shifted peak 8. Thus, the spectrum of the Co<sup>+</sup> complex gives strong indications of the presence of both ring-bound and O-bound acetophenone ligands in the ion population.

The overall quality of the Fe<sup>+</sup> spectrum is lower than for the other systems, making its interpretation more tentative. However, it seems most similar to the Co<sup>+</sup> spectrum, having some clear features (the peak at 1700 cm<sup>-1</sup> and the substantial dissociation around 1230 cm<sup>-1</sup>) that are indicative of ring-binding, in addition to displaying the diagnostic peaks for O-binding.

We continue the discussion of these spectra below, where we consider the comparisons of the experimental spectra with the DFT calculations. It is important to keep in mind that,

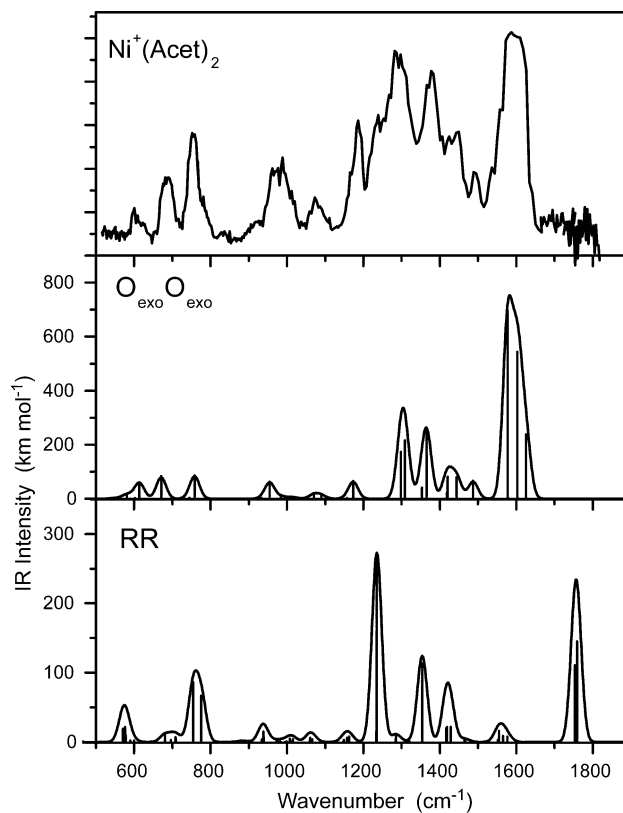


**Figure 4.** Experimental IRMPD spectrum and computed spectra of Ni<sup>+</sup>(acet)<sub>2</sub>.

although peak positions in IRMPD spectra are generally well correlated to those expected for single-photon, direct absorption spectra, the multiple photon nature of the IRMPD mechanism can cause discrepancies in the relative intensities of the peaks.<sup>37</sup> Thus, in the comparisons below, we consider quantitative agreement of peak positions to be most important and look only for qualitative similarity of predicted and observed intensity patterns.

**Spectroscopy of Ni(acet)<sub>2</sub><sup>+</sup>.** Figure 4 shows the spectrum of the Ni<sup>+</sup> bis complex along with predicted spectra of the OO and RR isomers. Based on the calculated spectra, diagnostic peaks for R-bound ligands, which are largely absent here, would be peaks at 1230 cm<sup>-1</sup> (red-shifted #8) and 1760 cm<sup>-1</sup> (#12). Interestingly, peak #3 does not seem useful for identifying R-bound ligands in this case. Diagnostic features for O-bound ligands are the very strong absorption on the blue side (1600–1650 cm<sup>-1</sup>) of the cluster of peaks near 1600 cm<sup>-1</sup> (red-shifted #12) and a peak near 1300 cm<sup>-1</sup> (blue-shifted #8). The predicted OR spectrum, not shown in this figure, is almost exactly a direct summation of the OO and RR spectra and shows both types of diagnostic peaks.

The absence of any peaks above 1600 cm<sup>-1</sup> in the experimental spectrum is a strong indication that no important fraction of the complexes have a ring-bound acetophenone ligand. The predicted spectra for the different OO-bound isomers (of which only the O<sub>exo</sub>O<sub>exo</sub> isomer is shown in Figure 4) all show good agreement with the IRMPD data. With one exception (see below), there is a good one-to-one correspondence of predicted and observed peaks, and the relative intensities are approximately matched. The immediate strong conclusion is the absence of a major extent of ring-bound acetophenone ligands. This is fully in accord with the expectation from the computations (Table 1) that O binding to Ni<sup>+</sup> is substantially more favorable than ring binding.

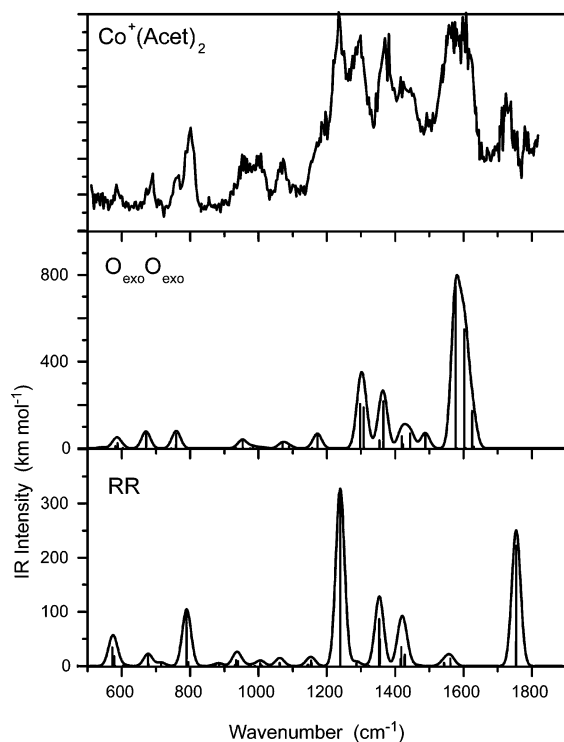


**Figure 5.** Observed spectrum for  $\text{Co}^+(\text{acet})_2$  and calculated spectra for the OO and RR isomeric possibilities.

The one feature not well matched in position in the calculated OO-bound spectra is the shoulder near  $1230\text{ cm}^{-1}$  in the experimental spectrum. (Compare with the clear absence of such a feature in the  $\text{Cr}^+$  spectrum in Figure 3.) There is a strong peak in the calculated spectrum of the OR and RR systems near this position, and thus, it is possible that the observed feature indicates the presence of a small population of ring-bound ligands. However, the absence of the expected corresponding peak above the baseline noise at  $1760\text{ cm}^{-1}$  sharply limits the maximum possible extent of such R-bound ligands, and we place an upper limit of  $\sim 10\%$  on the population of these isomers.

**Spectroscopy of  $\text{Co}(\text{acet})_2^+$ .** Figure 5 displays observed and calculated spectra of the  $\text{Co}^+$  bis complex. It is immediately obvious that neither the RR nor the OO prediction by itself gives a satisfactory match. The unique diagnostic peaks predicted for ring-bound ligands based on the calculations are the peaks at  $795$  (blue-shifted #3),  $1230$  (red-shifted #8), and  $1750\text{ cm}^{-1}$  (#12). The diagnostic peaks for O-bound ligands are the peaks at  $1600$  (red-shifted #12 plus #11, predicted to be very broad and intense) and  $1300\text{ cm}^{-1}$  (blue-shifted #8). Thus, the DFT spectra support our conclusion above based on the experimental data alone, that the IRMPD spectrum indicates the presence of both types of ligands. To the extent that the relative heights of the IRMPD peaks can be used to compare the relative amounts of the two types of ligand, it appears that R-bound and O-bound ligands are present in amounts that are not extremely dissimilar. This is nicely in accord with the computational thermochemistry, which predicts that ring binding and oxygen binding are not very different in energy for the  $\text{Co}^+$  system.

In principle, the presence of ring-bound ligands could mean that the complexes each have one ring-bound and one O-bound ligand, that OO and RR complexes are present together, or that all three isomers exist in the ion population. Figure 6 compares the observed spectrum to the DFT predicted spectrum for a homogeneous population of OR complexes, and the overall agreement is quite good. There is a one-to-one correspondence

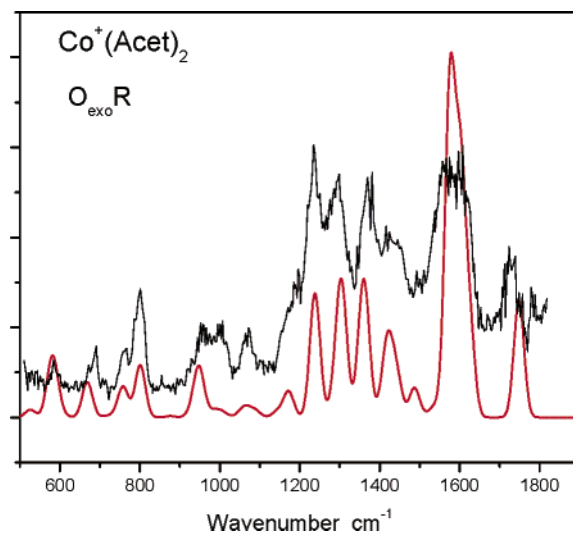


**Figure 6.** Comparison of the  $\text{Co}^+(\text{acet})_2$  spectrum with the computed  $\text{O}_{\text{exo}}\text{R}$  mixed-ligand complex, illustrating one of various combinations of an O-bound ligand with an R-bound ligand that give satisfactory fits to the observed spectrum.

of observed and predicted peaks, and the peak positions are well reproduced by the calculation, with the exception of the troublesome free-CO stretch, which is  $\sim 25\text{ cm}^{-1}$  too high in the predicted spectrum (see the Computational section above). Note that the calculation even reproduces the doubling of peak #3 in the IRMPD spectrum ( $750\text{--}800\text{ cm}^{-1}$ ). A predicted spectrum for an equal mixture of RR and OO, made by adding the calculated spectra of OO and RR with equal weight (not shown), is almost indistinguishable from the OR spectrum shown. Given that the hetero-dimer OR complex is somewhat more favorable thermochemically than a mixture of OO and RR homodimer complexes (see Table 1), a preponderance of OR complexes in the population seems likely, but there is really no way to make this distinction from the observed spectrum.

**Spectroscopy of  $\text{Fe}(\text{acet})_2^+$ .** Figure 7 shows observed and computed spectra for  $\text{Fe}^+(\text{acet})_2$ . The situation is similar to the  $\text{Co}^+$  case, with features in the spectrum indicating both R-bound and O-bound ligands, although the features suggesting R-bound ligands are weaker than in the spectrum of the  $\text{Co}^+$  complex. Note that the weak free carbonyl band near  $1710\text{ cm}^{-1}$  was reproducible from scan to scan and is unmistakably present in the single channel  $m/z = 176$  spectrum (see below). Also, the broad feature near  $1230\text{ cm}^{-1}$  is hard to explain in the absence of ring-bound ligands, as can be appreciated from the IRMPD spectrum of the exclusively OO-bound  $\text{Cr}^+(\text{acet})_2$  complexes in Figure 3.

The predicted  $\text{O}_{\text{exo}}\text{R}$  spectrum shown in Figure 7 gives a not unreasonable fit to the experimental spectrum, although the rather broad features of the latter make it hard to draw strong conclusions. A mixture of isomers is certainly also possible. The peaks attributable to R-bound ligands appear relatively weak in this case (compared, for instance, to the Co case). If we make the uncertain assumption that the IRMPD peak heights correspond to relative abundances, we can say that it is likely that at least some OO isomer is present to account for the apparent excess of O-bound ligands. The presence of R-bound ligands seems somewhat surprising in view of the calculated thermochemistry (Table 1), which predicts the OR and RR structures to be disfavored by substantial amounts of  $33$  and  $67\text{ kJ/mol}$ , respectively. However, as presented above, the experimental evidence for the presence of some fraction of ligands in the R-bound configuration seems strong. It seems quite possible

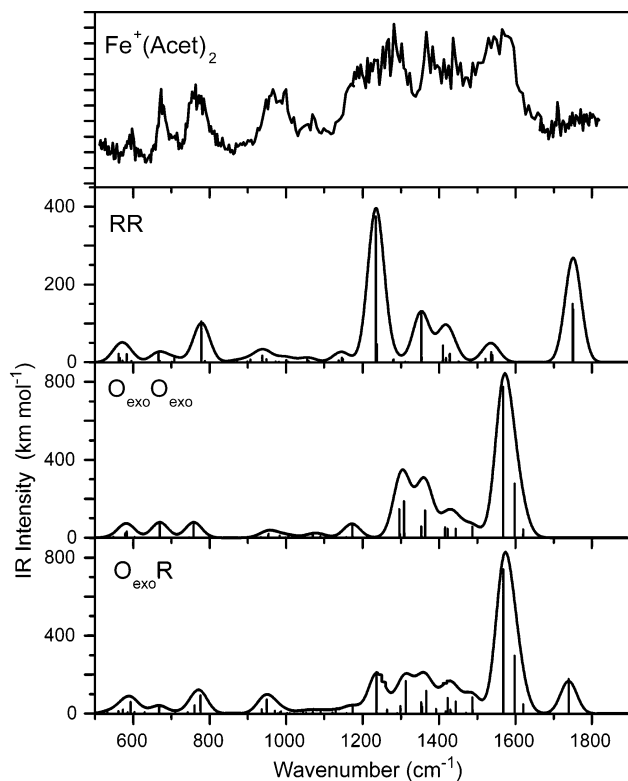


**Figure 7.** Observed spectrum for  $\text{Fe}^+(\text{acet})_2$  and calculated spectra for the OO, OR, and RR isomeric possibilities.

**TABLE 3: Calculated and Observed C=O Stretch Frequencies for the Mode with Highest Intensity of Each Type**

	$\nu(\text{O}_{\text{bound}})$			$\nu(\text{O}_{\text{unbound}})$		$\nu(\text{expt})$	
	OO	OR	rearr	RR	OR	bound <sup>a</sup>	unb
Ni	1626	1632	1643	1753	1750	1620	-
Co	1634	1647	1625	1754	1750	1620	1720
Fe	1567	1567	1645	1750	1739	1570	1710

<sup>a</sup> Assignment of the experimental position for metal-bound O is rather speculative, since this spectral region is overlapped by other vibrational modes. See text. “rearr” denotes the  $\text{M}^+(\text{acet})(\text{toluene})(\text{CO})$  rearranged structure. “ $\nu(\text{expt})(\text{bound})$ ” denotes the approximate position of the feature near  $1600\text{ cm}^{-1}$  that is assigned to the C=O stretching vibration of a metal-coordinated carbonyl oxygen. “ $\nu(\text{expt})(\text{unb})$ ” denotes the position of the peak assigned as the C=O stretching vibration of the unbound oxygen on a ring-coordinated acetophenone ligand.

that in this case a fraction of the ligands are kinetically trapped in an R-binding geometry which is strongly disfavored thermodynamically.

A notable and interesting feature of the  $\text{Fe}^+$  case is the shift to the red of the feature around  $1600\text{ cm}^{-1}$  or equivalently the absence of dissociation at frequencies higher than  $1610\text{ cm}^{-1}$ , in marked contrast to the other metal ion cases (Figure 3). This contrast indicates a distinctive character of the O-bound C=O stretching vibration in the  $\text{Fe}^+$  case, which is confirmed by the computational results. This C=O stretch is calculated in the vicinity of  $1620\text{ cm}^{-1}$  for the other metal ions (see Table 3) but is shifted to  $1570\text{ cm}^{-1}$  in the  $\text{Fe}^+$  case. Accordingly, we consider the strong dissociation seen around  $1600\text{--}1610\text{ cm}^{-1}$  in the  $\text{Cr}^+$ ,  $\text{Co}^+$ , and  $\text{Ni}^+$  cases as additional support for its assignment to the C=O stretching mode of O-bound ligands. In the  $\text{Fe}^+$  case, the predicted position of O-bound C=O around  $1570\text{ cm}^{-1}$  (Table 3) corresponds well to the maximum of the observed dissociation in this region, although this assignment is not very precise because of the extensive overlap and mixing

of the C=O stretch with the intense ring-deformation modes also around  $1550\text{--}1600\text{ cm}^{-1}$ .

We have no well developed explanation of why both experiment and computation show the C=O stretch of the  $\text{Fe}^+$ -bound carbonyl group to be red shifted to a markedly greater degree compared with the similar situation for the other metal ions. As a speculation, it may be important that  $\text{Fe}^+$  is the unique metal ion complex in this set for which the doubly occupied highest-lying d orbitals have  $d_{xy}$  or  $d_{x^2-y^2}$  character (taking the axis of quantization to be the metal–oxygen line). Quartet  $\text{Fe}^+$  has a valence configuration  $d_{\alpha}^5 d_{\beta}^2$ , denoting the fact that it has two d electrons outside the half-filled  $d^5$  shell. These two electrons are accommodated in the  $d_{xy}$  and  $d_{x^2-y^2}$  orbitals which minimize repulsion with the oxygen lone-pair electrons. On the other hand,  $\text{Co}^+$ , which is  $d_{\alpha}^5 d_{\beta}^3$ , and  $\text{Ni}^+$ , which is  $d_{\alpha}^5 d_{\beta}^4$  have their highest electrons in doubly occupied d orbitals of  $d_{x^2}$ ,  $d_{xz}$ , or  $d_{yz}$  shape, which have stronger repulsive interactions with the oxygen lone-pair orbitals. It is possible that  $\text{Fe}^+$  accordingly has the strongest electronic interaction with the carbonyl group, giving the largest red shift of the C=O stretch.

**Multiple Dissociation Channels.** When polyatomic molecules are excited to internal energies that are well above their dissociation thresholds, as in the IRMPD process, they are often observed to dissociate via multiple pathways, potentially having significantly different energies and accessing different parts of the potential energy surface.<sup>52–55</sup> The spectral responses in the different channels are observed to show slight differences, which are qualitatively discussed below. Despite these small discrepancies, it should be noted that the total fragment yield reflects the actual IRMPD spectrum of the parent ion and that this has been used in the spectral analyses of the previous sections.

Since the photon absorption rate can be much faster than the dissociation rate, one could picture a situation where the laser pulse instantaneously creates a particular internal energy distribution, which subsequently evolves on the excited-state potential energy surface and finds its way to one or more dissociative exit channels. Lifshitz was a leader in studying the success of statistical approaches to predicting the resulting fragmentation processes.<sup>56,57</sup> For electronic excitation, fast, nonstatistical dissociation processes seems to be possible as well as slow, statistical behavior (for example with peptides<sup>58,59</sup>), but with vibrational excitation as in IRMPD experiments, efficient energy randomization followed by statistically governed dissociation seems likely to predominate. The observed branching ratio then depends on the shape of the potential energy surface and on the internal energy distribution, which is sensitive to the spectral features of the molecule and to the fluence, wavelength, and bandwidth of the laser pulse. Studies where the multiple photon excitation process is modeled have shown that oddly shaped internal energy distributions may be generated,<sup>37</sup> and hence, it is very difficult to predict a priori the branching ratio at a given wavelength–fluence–bandwidth combination. In fact, fixed-wavelength IRMPD studies utilize this behavior to study branching ratios of activated reactions as a function of laser power and irradiation times.<sup>60–62</sup> Similarly, the relative yields into different dissociation channels may vary depending on the wavelength,<sup>37,63</sup> leading to qualitative differences between the IRMPD spectra recorded on different fragment mass channels.

Other, perhaps more straightforward effects that can occur and complicate the picture are as follows: (1) Vibrational anharmonicities can cause peaks to be shifted and broadened, the effects being more prominent in higher energy channels, and can also artificially enhance intensities of closely grouped

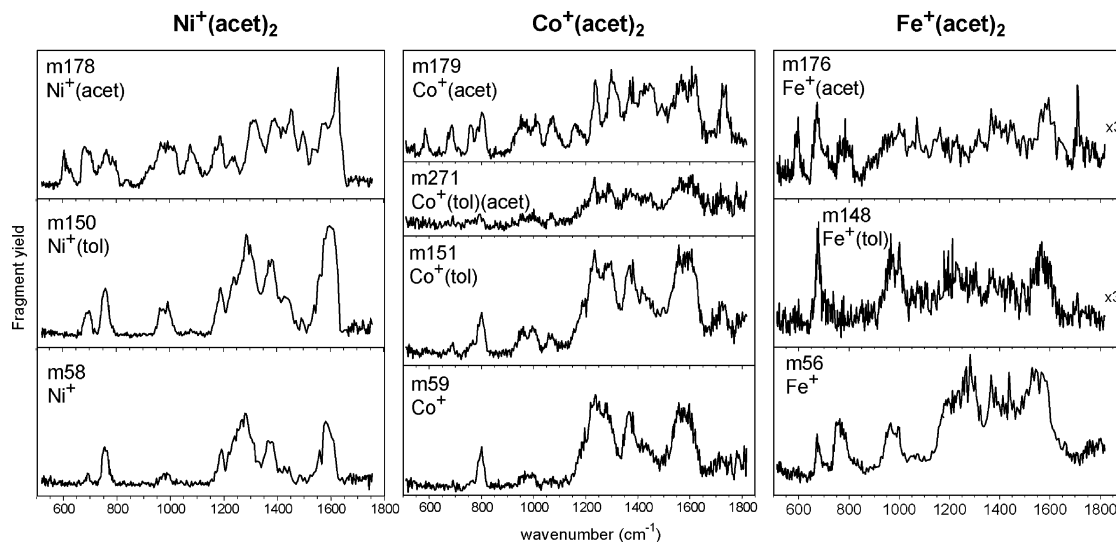


**Figure 8.** Action spectra for all individual dissociation channels of the three  $M^+(\text{acet})_2$  complexes studied. (The vertical scale is consistent among the set of plots for any given metal ion.)

peaks.<sup>37,63</sup> (2) Since the dissociation rate depends nonlinearly on the internal energy, weak peaks may be suppressed in higher energy dissociation channels. (3) Higher energy channels may be accessed via sequential steps, either rearrangements or dissociations, whereby an initial photoproduct (with a different IR spectrum) subsequently absorbs more photons (possibly within the same FELIX macropulse) and undergoes further dissociation. In this case the spectrum of the final product convolves the spectra of the parent and initial photoproduct.<sup>64</sup>

In addition to these considerations, the presence of multiple parent isomers can further complicate the situation.<sup>65</sup> However, note that, if the barriers separating the isomers are lower than the dissociation thresholds, rearrangement may occur before dissociation, in which case the observed yields into the different exit channels may not actually be different for the different isomers.

For all of the metal ion complexes studied here, multiple dissociation pathways were observed, including single and double ligand detachment and decarbonylation and a combination of both. Since simple ligand elimination from a metal center is expected to proceed via a barrierless or “loose” transition state,<sup>3</sup> one can reasonably expect the single ligand losses to be the channels having the lowest energy barriers to dissociation. Decarbonylation, yielding the  $M^+(\text{acet})(\text{toluene})$  product ion, is thermochemically lower in energy, but this rearrangement/dissociation is likely to have a significant barrier, so that its effective threshold energy is likely to be higher. Double ligand loss producing the bare metal ion is certainly the highest-energy channel. For all three bis-complexes studied here, qualitative differences between the IRMPD spectra in the different channels are observed, as can be seen in Figure 8.

Although the details vary from metal to metal, a few general trends can be observed. The spectra in the lowest-energy, single ligand loss channels are consistently the richest, having more and narrower peaks than the spectra in the higher energy channels. The spectra in the higher energy channels only show the strongest bands from the parent complexes, and these tend to be broadened and slightly redshifted with respect to the lower energy channels.

Quite striking is the disappearance of the feature near  $1760\text{ cm}^{-1}$  in the high-energy channels of the  $\text{Co}^+$  and  $\text{Fe}^+$  complexes. These peaks were considered highly specific to R-bound ligands and were considered in the discussion above

to correspond to OR complexes (having one R-bound and one O-bound ligand). This disappearance might reflect sequential-dissociation effects for the two-ligand loss process in the channel leading to bare metal ion. If the R-bound ligand leaves or changes binding geometry as the ion absorbs more photons, a situation could arise where the complex no longer absorbs photons at  $1760\text{ cm}^{-1}$  and does not acquire sufficient energy to drive off the second ligand at this wavelength. Alternatively, failure to pump the ion up to high internal energy could be due to a progressive red shift of this narrow, isolated peak.

#### Do the Ligands Undergo Intracomplex Decarbonylation?

Unlike the  $\text{Cr}^+$  complexes investigated in our earlier studies,<sup>7,34</sup> the ion–molecule chemistry of the complexes of acetophenone with  $\text{Fe}^+$ ,  $\text{Co}^+$ , and  $\text{Ni}^+$  is not necessarily limited to simple coordination of intact ligands. Up to this point, we have tacitly assumed that all of the parent complexes under investigation are normal coordination complexes of the metal ion with two intact acetophenone ligands, as was shown to be the case in the earlier  $\text{Cr}^+$  study.<sup>7</sup> However, the later transition metal ions are known to catalyze CO extrusion from carbonyl compounds, as has been reported for instance in a number of cases of decarbonylation of small ketones in ion–molecule reactions with late transition metal ions.<sup>39–41</sup> Acetophenone has not been studied from this point of view to our knowledge, but the formation of substantial amounts of decarbonylated mono- and bis-complex ions in the ion-formation process in the present experiments suggests that this is a facile fragmentation pathway for acetophenone complexes of  $\text{Fe}^+$ ,  $\text{Co}^+$ , and  $\text{Ni}^+$ . The expected decarbonylation product for acetophenone is toluene, and it will be assumed in the present discussion that ligands of composition  $\text{C}_7\text{H}_8$  are indeed toluene. Further consideration of this decarbonylation chemistry, and the spectroscopic confirmation of toluene in decarbonylated complexes, will be presented in another publication.<sup>36</sup>

For the present purposes, the point is that attack on the acetophenone ligand by these metal ions resulting in CO extrusion from acetophenone is a facile rearrangement process. It is a serious possibility that some fraction of the parent complexes have undergone a decarbonylation reaction and have become trapped in the “product-side” potential energy well as a ternary complex of the metal ion with CO, toluene, and an intact acetophenone ligand. The computed thermochemistry indicates that such ternary complexes are significantly more



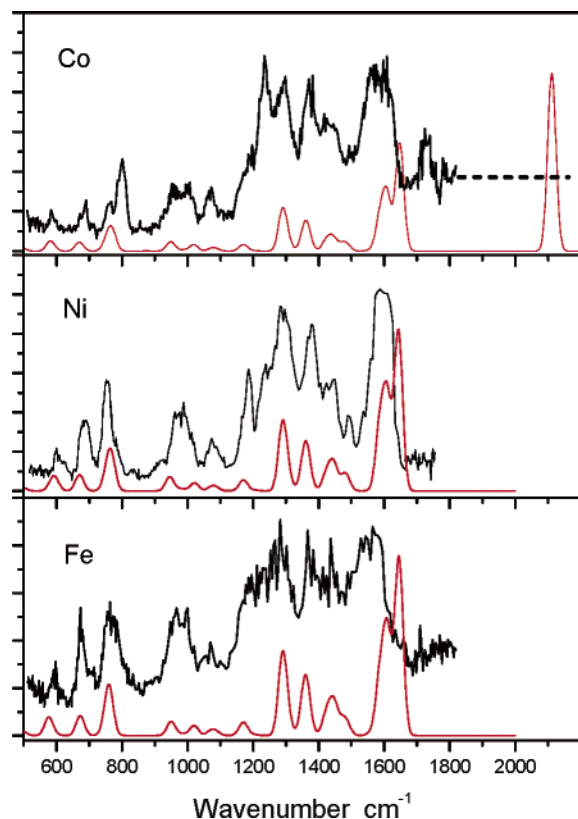


**Figure 9.** Computed spectra of  $M^+(\text{O}_{\text{exo-acet}})(\text{toluene})(\text{CO})$  complexes (red), compared with experimental IRMPD spectra (black).

stable than the unrearranged bis-acetophenone complexes for  $\text{Co}^+$  and  $\text{Fe}^+$  (see Table 1) and that they are comparable in energy for  $\text{Ni}^+$ . In addition, the  $\text{Co}^+$  complexes seem a particularly likely candidate for such a reaction, since they are unique in showing the CO-loss product ( $m/z = 271$ ) as an IRMPD photofragment (see Figure 8), which could indicate (although it does not require) that the departing CO already exists as an independent ligand in the complex prior to photoactivation.

Figure 9 shows the experimental IRMPD spectra for the complexes studied here, along with the calculated spectra for the ternary complexes described above, assuming O-bound acetophenone ligands as indicated by the DFT thermochemistry (see Table 1). Any such complexes should have a clear spectroscopic signature, since the stretching vibration of the CO ligand would appear in the 2000–2200  $\text{cm}^{-1}$  region. This region was examined carefully for the  $\text{Co}^+$  complex, as shown in the top panel. Although this region was not scanned continuously, a careful stepwise search was performed using FELIX in 3rd harmonic mode, taking 0.05  $\mu\text{m}$  steps and averaging 50 mass spectra at each point, so that even a small amount of photo-dissociation could be detected. None was observed, however, as indicated by the broken line in the figure, and this virtually eliminates the possibility of any free CO ligands existing in the parent  $\text{Co}^+$  complexes, especially since this mode is quite intense in the calculated spectrum.

The 2000–2200  $\text{cm}^{-1}$  region was not explicitly searched for the  $\text{Ni}^+$  and  $\text{Fe}^+$  systems, but we do not consider it likely that these cases are different from the  $\text{Co}^+$  case. For one thing (Table 1), these complexes have less enthalpic driving force toward the ternary rearrangement products than for the  $\text{Co}^+$  case. Moreover, the O-bound acetophenone CO-stretching vibrations are calculated to lie near 1640  $\text{cm}^{-1}$  in the predicted spectra of the rearranged ternary complexes, which is significantly farther

to the blue than is calculated for the unrearranged bis complexes and does not fit at all well to the observed features in this region (Figure 9). Thus, we conclude that the putative “product side” ternary complexes described above were not formed as a significant part of the parent-ion populations in these experiments.

**Spin State Considerations.** A notable finding in the study of ring-bound bis complexes of aromatic ligands with  $\text{Cr}^+$  was that the spectra gave a clear and graphic confirmation of the switch from high-spin character of the mono complex to low-spin character of the bis complex.<sup>7</sup> It may be interesting to consider the possible similar exploitation of the present spectra for spin-state characterization. With  $\text{Fe}^+$  and  $\text{Co}^+$ , there are possibilities that the strong ligand field of an RR-bound bis complex might induce a spin conversion to a low-spin electronic state (doublet for  $\text{Fe}^+$ , singlet for  $\text{Co}^+$ ). However, the advantage of doing so is not as evident as in the  $\text{Cr}^+$  case. In the latter case, going from the sextet to the doublet removes both of the repulsive electrons in the  $d_{xz}$  and  $d_{yz}$  orbitals, placing them in favorable,  $d \rightarrow \pi^*$  donating orbitals of  $d_{xy}$  and  $d_{x^2-y^2}$  shape. In the  $\text{Fe}^+$  case, going from the quartet to the doublet moves only one electron to a more favorable orbital, whereas in the  $\text{Co}^+$  case, going from the triplet state to the singlet state gives no qualitative improvement in the electronic configuration at all.

Since there is at least some basis for suspecting a spin flip to low-spin RR bis complexes for  $\text{Fe}^+$ , it is worth thinking about this case a little more closely. The energy cost of promoting the bare atomic  $\text{Fe}^+$  ion from the  $^4\text{F}$  ( $d^7$ ) state to the  $^2\text{G}$  ( $d^7$ ) state is 167 kJ/mol.<sup>66</sup> This is actually less than the energy cost of promoting  $\text{Cr}^+$  from the sextet to the doublet state (311 kJ/mol), so this is a reasonable promotion on energetic grounds. As indicated in Table 1, the calculations actually show the low-spin doublet state of the  $\text{Fe}^+$  RR complex to be not very different in energy from the quartet state. However, the OO complex, with a weaker ligand field, is calculated to favor the quartet state strongly, by 146 kJ/mol, and the OR complex is also calculated to favor the quartet state strongly, by 82 kJ/mol. The calculated spectra of the quartet and doublet spin states of the RR complex are almost indistinguishable, and it would not be possible to assign the spin state for complexes with R-bound ligands from the spectra, even given a higher-quality experimental spectrum than was available. However, since there seems little likelihood of much presence of RR complexes in the actual population, and since the OR and OO complexes strongly favor the quartet state on energy grounds, it seems likely that essentially all of the  $\text{Fe}^+$  complexes observed here are quartets.

We did not succeed in obtaining a converged singlet-state calculation of the  $\text{Co}^+(\text{acet})_2$  complex. There seems no reason to expect such complexes to be energetically competitive with the triplet states, and this effort was not pursued very far.

## Conclusions

IRMPD spectra of good quality were obtained for the  $\text{Co}^+$  and  $\text{Ni}^+$  bis-complexes, and these provide an interesting contrast.  $\text{Co}^+(\text{acet})_2$  has important fractions of both R- and O-bound ligands. The observed spectrum is equally consistent with the OR structure or with a mixture of similar fractions of OO and RR complexes, but it was thought most likely (based on the thermochemistry) to be predominantly the OR structure. Rearrangement of the ligand through oxidative insertion of the metal ion into a C–C bond followed by closing up to toluene plus CO is thermochemically highly favorable for  $\text{Co}^+$ . However, conversion of any significant part of the population to  $\text{Co}^+(\text{acet})(\text{toluene})(\text{CO})$  was ruled out spectroscopically based

on the absence of a CO stretching peak corresponding to metal-bound CO, as well as an unsatisfactory fit in the acetophenone C=O stretching region.

In contrast to the Co<sup>+</sup> situation, the Ni<sup>+</sup>(acet)<sub>2</sub> spectrum was inconsistent with the presence of more than a small fraction (not more than ~10%) of R-bound acetophenone ligands. The spectrum indicated a predominant population of OO structures, and was quite similar to the previously reported spectrum of Cr<sup>+</sup>(acet)<sub>2</sub>, also assigned as reflecting OO binding. The absence of R-bound ligands was in line with the unfavorable computed thermochemistry of ring- $\pi$  binding versus side-chain O binding for this metal ion. Substantial conversion to the Ni<sup>+</sup>(acet)-(toluene)(CO) structure was not in very good accord with the spectrum, but was not completely ruled out spectroscopically. However, conversion to such a rearranged structure was further considered unlikely based on the lack of a strong thermochemical driving force to rearrangement.

The ability of ring  $\pi$  binding to compete successfully with O-binding in the Co<sup>+</sup>(acet)<sub>2</sub> complex reflects the exceptional affinity of Co<sup>+</sup> for the ring site of benzene-derived substrates. The Ni<sup>+</sup> and Cr<sup>+</sup> bis complexes offer a notable contrast to Co<sup>+</sup>, in that they strongly prefer oxygen binding of the metal ion. In terms of electronic configurations, the former two ions are characterized by a HOMO of d<sub>xz</sub> or d<sub>yz</sub> shape which has strongly repulsive interactions with the ring  $\pi$  electrons. This disfavors binding to the ring  $\pi$  system and leads to a preponderance of ligand binding on the oxygen site.

The overall similarity of the Fe<sup>+</sup>(acet)<sub>2</sub> spectrum to that of the Co<sup>+</sup> complex indicated a bis-complex with observable fractions of both R-bound and O-bound ligands, although probably less R-bound ligands than the Co<sup>+</sup> case. The OR structure gave a possible fit to the spectrum, but it is likely that less than half of the ligands are actually R bound in this population. The presence of R-bound ligands was considered surprising in light of the unfavorable thermochemistry but appeared necessary in order to account for the spectrum. It is possible that some ions in the population are kinetically trapped in the thermodynamically disfavored OR or RR geometry. Rearrangement to the Fe<sup>+</sup>(O-acet)(toluene)(CO) structure could be ruled out convincingly on the basis of the 1600 cm<sup>-1</sup> region of the spectrum. An interesting result, shown both in the experimental spectrum and in the computations, was that the C=O stretching mode of O-bound Fe<sup>+</sup> complexes was significantly more red shifted (of the order of 40–50 cm<sup>-1</sup> farther to the red) than for Cr<sup>+</sup>, Co<sup>+</sup>, or Ni<sup>+</sup>. This result may be related to the unique electronic configuration of the frontier d orbitals of quartet Fe<sup>+</sup>.

Ligand-field induced spin change from quartet to doublet in the Fe<sup>+</sup> case was considered to be thermochemically possible for RR complexes but would not be spectroscopically distinguishable. In any case, the fraction of RR complexes for this metal ion is at best not very large, and the OR and OO complexes are probably quartets. Spin reduction in the Co<sup>+</sup> complexes is not likely.

**Acknowledgment.** This work is part of the research program of FOM, which is financially supported by the Nederlandse Organisatie voor Wetenschappelijk Onderzoek (NWO). We acknowledge the FELIX staff for their excellent support. R.C.D. acknowledges the support of the donors of the Petroleum Research Fund, administered by the American Chemical Society, and travel support from the National Science Foundation. This paper is dedicated to the memory of Chava Lifshitz, a dear friend and superlative scientist.

## References and Notes

- (1) Bauschlicher, C. W.; Partridge, H.; Langhoff, S. R. *J. Phys. Chem.* **1992**, *96*, 3273.
- (2) Jaeger, T. D.; van Heijnsbergen, D.; Klippenstein, S. J.; von Helden, G.; Meijer, G.; Duncan, M. A. *J. Am. Chem. Soc.* **2004**, *126*, 10981.
- (3) Meyer, F.; Khan, F. A.; Armentrout, P. B. *J. Am. Chem. Soc.* **1995**, *117*, 9740.
- (4) Rodgers, M. T.; Armentrout, P. B. *Mass Spectrom. Rev.* **2000**, *19*, 215.
- (5) Yang, C.-N.; Klippenstein, S. J. *J. Phys. Chem. A* **1999**, *103*, 1094.
- (6) Dunbar, R. C. *J. Phys. Chem. A* **2002**, *106*, 7328.
- (7) Moore, D. T.; Oomens, J.; Eyler, J. R.; von Helden, G.; Meijer, G.; Dunbar, R. C. *J. Am. Chem. Soc.* **2005**, *127*, 7243.
- (8) Eller, K.; Schwarz, H. *Chem. Rev.* **1991**, *91*, 1121.
- (9) *Organometallic Ion Chemistry*; Freiser, B. S., Ed.; Kluwer: Dordrecht, The Netherlands, 1996.
- (10) Leary, J. A.; Armentrout, P. B. *Int. J. Mass Spectrom.* **2001**, *204*, 1387.
- (11) *Gas-Phase Inorganic Chemistry*; Russell, D. H., Ed.; Plenum: New York, 1989.
- (12) DeWall, S. L.; Meadows, E. S.; Barbour, L. J.; Gokel, G. W. *Proc. Natl. Acad. Sci.* **2000**, *97*, 6271.
- (13) Dougherty, D. A. *Science* **1996**, *271*, 163.
- (14) Gallivan, J. P.; Dougherty, D. A. *Proc. Natl. Acad. Sci.* **1999**, *96*, 9459.
- (15) Hu, J.; Barbour, L. J.; Gokel, G. W. *Proc. Natl. Acad. Sci.* **2002**, *99*, 5121.
- (16) Minoux, H.; Chipot, C. *J. Am. Chem. Soc.* **1999**, *121*, 10366.
- (17) Blomberg, M. R. A.; Siegbahn, P. E. M.; Babcock, G. T. *J. Am. Chem. Soc.* **1998**, *120*, 8812.
- (18) Pierloot, K.; de Kerpel, J. O. A.; Ryde, U.; Olsson, M. H. M.; Roos, B. O. *J. Am. Chem. Soc.* **1998**, *120*, 13156.
- (19) Metcalfe, C.; Thomas, J. A. *Chem. Soc. Rev.* **2003**, *32*, 215.
- (20) Gnjec, A.; Fonte, J. A.; Atwood, C.; Martins, R. N. *Front. Biosci.* **2002**, *7*, d1016.
- (21) Ming, L.-J.; Epperson, J. D. *J. Inorg. Biochem.* **2002**, *91*, 46.
- (22) Satterfield, M.; Brodbelt, J. S. *Inorg. Chem.* **2001**, *40*, 5393.
- (23) Jaeger, T. D.; Duncan, M. A. *Int. J. Mass Spectrom.* **2005**, *241*, 165.
- (24) Kapota, C.; Lemaire, J.; Maître, P.; Ohanessian, G. *J. Am. Chem. Soc.* **2004**, *126*, 1836.
- (25) LeCaër, S.; Heninger, M.; Lemaire, J.; Boissel, P.; Maître, P.; Mestdagh, H. *Chem. Phys. Lett.* **2004**, *385*, 273.
- (26) Lemaire, J.; Boissel, P.; Heninger, M.; Mauclair, G.; Bellec, G.; Mestdagh, H.; Simon, A.; LeCaër, S.; Ortega, J. M.; Glotin, F.; Maître, P. *Phys. Rev. Lett.* **2002**, *89*, 273002.
- (27) Moore, D. T.; Oomens, J.; van der Meer, L.; von Helden, G.; Meijer, G.; Valle, J.; Marshall, A. G.; Eyler, J. R. *ChemPhysChem* **2004**, *5*, 740.
- (28) Moore, D. T.; Oomens, J.; Eyler, J. R.; von Helden, G.; Meijer, G.; Ridge, D. P. *J. Am. Chem. Soc.* **2004**, *126*, 14726.
- (29) Polfer, N. C.; Oomens, J.; Moore, D. T.; von Helden, G.; Meijer, G.; Dunbar, R. C. *J. Am. Chem. Soc.* **2006**, *128* (2), 517–525.
- (30) Reinhard, B. M.; Lagutschenkov, A.; Lemaire, J.; Maître, P.; Boissel, P.; Niedner-Schatteburg, G. *J. Phys. Chem. A* **2004**, *108*, 3350.
- (31) Simon, A.; Jones, W.; Ortega, J.-M.; Boissel, P.; Lemaire, J.; Maître, P. *J. Am. Chem. Soc.* **2004**, *126*, 11666.
- (32) Walker, N. R.; Walters, R. S.; Pillai, E. D.; Duncan, M. A. *J. Chem. Phys.* **2003**, *119*, 10471.
- (33) Walters, R. S.; Jaeger, T. D.; Duncan, M. A. *J. Phys. Chem. A* **2002**, *106*, 10482.
- (34) Oomens, J.; Moore, D. T.; von Helden, G.; Meijer, G.; Dunbar, R. C. *J. Am. Chem. Soc.* **2004**, *126*, 724.
- (35) van Heijnsbergen, D.; von Helden, G.; Meijer, G.; Maître, P.; Duncan, M. A. *J. Am. Chem. Soc.* **2002**, *124*, 1562.
- (36) Moore, D. T.; Oomens, J.; Dunbar, R. C. **2005**, in preparation.
- (37) Oomens, J.; Tielens, A. G. G. M.; Sartakov, B.; von Helden, G.; Meijer, G. *Astrophys. J.* **2003**, *591*, 968.
- (38) Bagratashvili, V. N.; Letokhov, V. S.; Makarov, A. A.; Ryabov, E. A. *Multiple Photon Infrared Laser Photophysics and Photochemistry*; Harwood Academic Publishers: Chichester, U.K., 1985.
- (39) Halle, L. F.; Crowe, W. E.; Armentrout, P. B.; Beauchamp, J. L. *Organometallics* **1984**, *3*, 1694.
- (40) Carpenter, C. J.; von Koppen, P. A. M.; Bowers, M. T. *J. Am. Chem. Soc.* **1995**, *117*, 10976.
- (41) Burnier, R. C.; Byrd, G. D.; Freiser, B. S. *J. Am. Chem. Soc.* **1981**, *103*, 4360.
- (42) Surjasasmita, P. I.; Freiser, B. S. *J. Am. Soc. Mass Spectrom.* **1993**, *4*, 135.
- (43) Schröder, D.; Eller, K.; Prusse, T.; Schwarz, H. *Organometallics* **1991**, *10*, 2052.
- (44) Larsen, B. S.; Ridge, D. P. *J. Am. Chem. Soc.* **1984**, *106*, 1912.

- (45) Valle, J.; Oomens, J.; Moore, D. T.; von Helden, G.; Hendrickson, C. L.; Blakney, G. T.; van der Meer, A. F. G.; Marshall, A. G. *Rev. Sci. Instrum.* **2005**, *76*, 023103.
- (46) Dunbar, R. C. *Mass Spectrom. Rev.* **1992**, *11*, 309.
- (47) Kang, H.; Beauchamp, J. L. *J. Chem. Phys.* **1985**, *89*, 3364.
- (48) Marshall, A. G.; Hendrickson, C. L.; Jackson, G. S. *Mass Spectrom. Rev.* **1998**, *17*, 1.
- (49) Frisch, M. J.; Trucks, G. W.; Schlegel, H. B.; Scuseria, G. E.; Robb, M. A.; Cheeseman, J. R.; Montgomery, J. A., Jr.; Vreven, T.; Kudin, K. N.; Burant, J. C.; Millam, J. M.; Iyengar, S. S.; Tomasi, J.; Barone, V.; Mennucci, B.; Cossi, M.; Scalmani, G.; Rega, N.; Petersson, G. A.; Nakatsuji, H.; Hada, M.; Ehara, M.; Toyota, K.; Fukuda, R.; Hasegawa, J.; Ishida, M.; Nakajima, T.; Honda, Y.; Kitao, O.; Nakai, H.; Klene, M.; Li, X.; Knox, J. E.; Hratchian, H. P.; Cross, J. B.; Bakken, V.; Adamo, C.; Jaramillo, J.; Gomperts, R.; Stratmann, R. E.; Yazyev, O.; Austin, A. J.; Cammi, R.; Pomelli, C.; Ochterski, J. W.; Ayala, P. Y.; Morokuma, K.; Voth, G. A.; Salvador, P.; Dannenberg, J. J.; Zakrzewski, V. G.; Dapprich, S.; Daniels, A. D.; Strain, M. C.; Farkas, O.; Malick, D. K.; Rabuck, A. D.; Raghavachari, K.; Foresman, J. B.; Ortiz, J. V.; Cui, Q.; Baboul, A. G.; Clifford, S.; Cioslowski, J.; Stefanov, B. B.; Liu, G.; Liashenko, A.; Piskorz, P.; Komaromi, I.; Martin, R. L.; Fox, D. J.; Keith, T.; Al-Laham, M. A.; Peng, C. Y.; Nanayakkara, A.; Challacombe, M.; Gill, P. M. W.; Johnson, B.; Chen, W.; Wong, M. W.; Gonzalez, C.; Pople, J. A. *Gaussian 03*; Gaussian, Inc.: Wallingford, CT, 2004.
- (50) NIST Mass Spec Data Center, S. E. Stein, director, "Infrared Spectra" in NIST Chemistry WebBook, NIST Standard Reference Database Number 69; Linstrom, P. J., Mallard, W. G., Eds.; March 2003, National Institute of Standards and Technology, Gaithersburg MD, 20899 (<http://webbook.nist.gov>).
- (51) Li, Y.; Baer, T. *J. Chem. Phys. A* **2002**, *106*, 9820.
- (52) Baer, T.; Hase, W. L. *Unimolecular Reaction Dynamics: Theory and Experiments*; Oxford University Press: New York, 1996.
- (53) Holbrook, K. A.; Pilling, M. J.; Robertson, S. H. *Unimolecular Reactions*; Wiley: New York, 1996.
- (54) Gilbert, R. G.; Smith, S. C. *Theory of Unimolecular and Recombination Reactions*; Blackwell: Oxford, 1990.
- (55) Armentrout, P. B. *Top. Curr. Chem.* **2003**, *225* (Modern Mass Spectrometry), 233.
- (56) Lifshitz, C. *J. Phys. Chem.* **1983**, *87*, 2304.
- (57) Lifshitz, C. *Adv. Mass Spectrom.* **1989**, *11A*, 713.
- (58) Hu, Y.; Hadas, B.; Davidovitz, M.; Balta, B.; Lifshitz, C. *J. Phys. Chem. A* **2003**, *107*, 6507.
- (59) Weinkauff, R.; Schanen, P.; Metsala, A.; Schlag, E. W.; Burgle, M.; Kessler, H. *J. Phys. Chem.* **1996**, *100*, 18567.
- (60) Bomse, D. S.; Beauchamp, J. L. *J. Am. Chem. Soc.* **1981**, *103*, 3292.
- (61) Moylan, C. R.; Brasinsk, J. R.; Brauman, J. I. *Chem. Phys. Lett.* **1983**, *98*, 1.
- (62) Zhao, X. S.; Hints, E. J.; Lee, Y. T. *J. Chem. Phys.* **1988**, *88*, 801.
- (63) Oomens, J.; Moore, D. T.; Meijer, G.; von Helden, G. *Phys. Chem. Chem. Phys.* **2004**, *6*, 710.
- (64) Moore, D. T.; Oomens, J.; Eyler, J. R.; Meijer, G.; von Helden, G. **2005**, in preparation.
- (65) Polfer, N.; Valle, J. J.; Moore, D. T.; Oomens, J.; Eyler, J. R.; Bendiak, B. *Anal. Chem.* **2006**, *78*, 670.
- (66) NIST Atomic Spectra Database (version 2.0). [Online] Available: <http://physics.nist.gov/asd2> [September 19, 2005]. National Institute of Standards and Technology, Gaithersburg, MD.